JOURNAL OF GEOPHYSICAL RESEARCH, VOL. 93, NO. B6, PAGES 6477–6484, JUNE 10, 1988

Postshock Temperatures in Silica

M. B. BOSLOUGH

Sandia National Laboratories, Albuquerque, New Mexico

Experimental postshock temperatures for crystalline quartz released from shock states between 86 and 127 GPa and for fused silica released from 59 to 73 GPa have been determined using previously measured spectral radiance data. The temperatures range from 3660 to 4150 K and are consistent with the interpretation based on shock temperature measurements, that the Hugoniot of SiO_2 crosses the phase boundary between stishovite and liquid. The new postshock temperatures were used to determine the Grüneisen parameter of liquid silica at high pressures and temperatures and the specific volume of the release state ($\gamma/V = 3.5$ Mg/m^3 and $V_r = 0.266$ m^3/Mg, respectively), although there is some ambiguity as to whether this volume corresponds to a partial or total release state. To show the validity of these postshock temperatures, a radiative transport model was extended to times after free surface arrival of the shock wave.

INTRODUCTION

Silicate minerals are the most abundant constituents of the Earth's crust and mantle. Of these, silica is the simplest and most studied. Knowledge of the behavior of SiO_2 at high pressures and temperatures is critical to the understanding of the Earth's interior, as well as that of the severe states produced by high-pressure shocks due to impacts and nuclear explosions. *Wackerle* [1962] used planar explosive loading techniques to generate strong shocks in quartz and measured shock velocities, thereby determining pressure-volume states. His data strongly suggested the transformation to stishovite, a dense high-pressure phase in the rutile structure, at shock pressures above 14 GPa. *McQueen et al.* [1963] used Wackerle's data to construct the first equation of state of stishovite. *Lyzenga et al.* [1983] recognized the importance of measuring shock temperatures in order to determine the thermal component of the high-pressure equation of state. They developed a radiation pyrometer and measured temperatures of shocked silica at pressures from 60 to 140 GPa. They inferred from their data that the melting curve of stishovite passes through the Hugoniots of fused silica and α quartz with a melting temperature of 4500 K at a pressure of 70 GPa. *Chhabildas and Miller* [1985] used velocity interferometric techniques to determine release paths of shocked quartz from pressures between 15 and 110 GPa. Their data suggest that the final state upon release of quartz from shock pressures above 50 GPa is a high-density liquid silica.

Postshock temperatures are the residual temperatures existing in a material after the passage of a shock and then an unloading wave. Postshock temperatures are typically calculated using Hugoniot data with an independently calculated shock temperature and assuming a Mie-Grüneisen equation of state and isentropic decompression. For silica the shock temperatures and release paths have both been measured directly, so if there were no phase changes and if the Mie-Grüneisen and isentropic release assumptions are valid, the postshock temperatures could be determined exactly. Alternatively, measured postshock temperatures can be used to constrain parameters associated with any phase change along the release path, as well as to check the validity of the assumptions. The only existing measurements of postshock temperatures in silica were carried out by *Raikes and Ahrens* [1979], who used infrared detectors to determine brightness temperatures. Their experiments only achieved shock pressures of less than 21.5 GPa, which was not high enough to probe the inferred stishovite/melt phase boundary in the shocked state. The present study makes use of the spectral radiance data for shocked silica by *Lyzenga* [1980] to determine experimental postshock temperatures. This is the same data used to calculate the shock temperatures published by *Ahrens et al.* [1982] and *Lyzenga et al.* [1983].

Paper number 7B1056.
0148-0227/88/007B-1056$05.00

EXPERIMENTAL PROCEDURE

A description of how the postshock temperatures were determined requires a brief discussion of how *Lyzenga*'s [1980] experiments were performed. SiO_2 samples were shocked to pressures ranging from 59 to 137 GPa by the impact of projectiles launched at high velocity using the Lawrence Livermore National Laboratory two-stage light-gas gun. The intensity of light radiated from shocked SiO_2 was measured at six different wavelengths with the six-channel radiation pyrometer of *Lyzenga and Ahrens* [1979]. A typical oscilloscope trace is shown in Figure 1. The measurements were made by focusing the image of the free surface of the initially transparent samples on each of six photodiodes with a different wavelength interference filter in each light path. The original purpose of the experiments was to measure the temperature of shocked SiO_2. This information is carried by the spectral radiance at the time the shock wave reaches the free surface of the sample. We can show by a simple radiation transport model along with a few simplifying assumptions that the subsequent spectral radiance history carries information about the residual, or postshock temperature of SiO_2. This model is not necessary to determine the postshock temperatures but is presented in order to demonstrate that meaningful temperatures can in principle be determined from postshock spectral radiance measurements.

It is important to demonstrate that the observed portion of the shocked samples remain under uniaxially strained conditions for a significant length of time after the shock breaks out at the free surface. The optical system of the *Lyzenga and Ahrens* [1979] pyrometer demagnifies the image of the 17-mm-diameter target by a factor of 0.37, so the 1-mm square photodiode active area collects light from a 2.7-mm square area of the target. For a well-centered target, this observed area lies within a circle with a 2-mm radius. An edge rarefac-

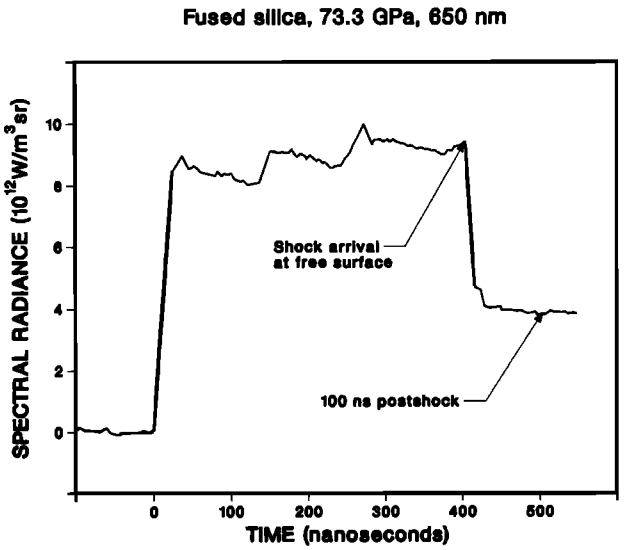

Fig. 1. Record of shock-induced spectral radiance (at $\lambda = 650$ nm) versus time, for fused silica shock-loaded to 73.3 GPa [*Lyzenga et al.*, 1983]. First arrow marks the time of shock arrival at the free surface, when records were read to determine shock temperatures. Second arrow marks time 100 ns later, when records were read to determine postshock temperatures.

tion must therefore travel at least 6.5 mm before it interferes with this zone. A rarefaction velocity of 14 km/s into fused silica shocked to 97.5 Gpa was measured by *Lyzenga et al.* [1983], so a minimum of 450 ns of observation time is allowed. The corresponding 9.2 km/s shock would transit a 3-mm-thick sample in about 325 ns, so the region observed 100 ns after shock breakout is still under uniaxial strain. The time window is even longer for observations of the free surface, since the sound velocity is significantly lower in that portion of the sample that has already released to low pressure by a free-surface unloading wave. A similar argument can be made for silica shocked to lower peak pressures; the shock velocity is lower, but the release wave velocity is also lower. The validity of the uniaxial strain assumption can be shown for crystalline quartz using the release wave velocities of *Chhabildas and Miller* [1985]. For a detailed discussion of radial stress release phenomena in plate impact experiments, the reader is referred to *Stevens and Jones* [1972].

It is also important to consider possible sources of light contamination. *Nicol et al.* [1988] observed that spurious light emission from the environment around the target (probably due to gas blow-by past the projectile) can enter the optical system. The possible effect on the postshock measurements is more of a concern than for shock measurements, since postshock intensities are lower than shock intensities and because the chance that spurious light will enter the pyrometer increases with time. However, there is evidence from earlier data that the relative intensity of any spurious light emission is small compared to the intensities giving rise to the present temperature measurements. Data of *Lyzenga and Ahrens* [1979] on silver/sapphire composite targets show that light intensities return to their baseline values 100 to 200 ns after shock arrival at the sapphire free surface. Also, peak spectral radiances measured by *Lyzenga* [1980] from shocked water are less than half the values of the lowest spectral radiance values used in the present paper, at a given wavelength. While light emission from an expanding vapor cloud is a possible source of error, there is no evidence that it is bright enough to interfere with the present measurements.

RADIATIVE TRANSPORT MODEL

As described by *Boslough* [1985], the time dependence in the spectral radiance, at a given wavelength, of light radiated from a sample undergoing shock compression is given by

$$I(t) = r\{\varepsilon_i{}^0 f[T_i(t)] \exp[-a_s(U_s-u_p)t] \exp[-a_u(d-U_s t)] + f(T_s)[1-\exp(-a_s(U_s-u_p)t)] \exp[-a_u(d-U_s t)]\} \quad (1)$$

where $f(T)$ is the Planck distribution function, T_s is the temperature of the shocked material, $T_i(t)$ is the (time dependent) temperature of the interface between the sample and opaque flyer or driver plate, t is time after shock arrival at the interface, d is sample thickness, U_s and u_p are shock and particle velocities, respectively, in the shocked material, a_s and a_u are absorption coefficients of shocked and unshocked sample material, respectively, $\varepsilon_i{}^0$ is the intrinsic emissivity of the interface, and r is a reduction factor which accounts for internal reflections. This equation assumes that the temperature of the unshocked sample is low enough that no light is radiated and that the reflectivity of the sample-driver interface is negligible. It is valid for times between shock arrival at the interface and at the free surface ($0 < t < d/U_s$). The first term describes light radiated from the interface, and the second term describes light radiated from the shocked sample. In order to extend the equation to times greater than d/U_s, a third term is required which describes light radiated from material that has been released from the shocked state. The release state has a corresponding (postshock) temperature T_r and absorption coefficient a_r. In general, release waves are dispersive and therefore cannot be represented by a single velocity. Within the release wave, there is a gradient of disturbance velocities, particle velocities, pressures, and hence temperatures. For simplicity, we will consider the rarefaction to be a discontinuity traveling at speed U_r. We could also invoke the free surface approximation [e.g., *Rice et al.*, 1958] in which the free surface velocity, and therefore the particle velocity of the release state, is $2u_p$. However, because the evidence suggests that the material is going through a phase change this is probably not a good assumption, so to keep the equations general, we can call the free surface velocity u_{fs} and not make any assumptions as to its value. For times in the interval

$$d/U_s < t < d\left(1-\frac{u_p}{U_s}\right)\Big/U_r$$

we get

$$I(t) = r'\{\varepsilon_i{}^0 f[T_i(t)] \exp[-a_s\delta_s(t)] \exp[-a_r\delta_r(t)] + f(T_s)[1-\exp(-a_s\delta_s(t))] \exp[-a_r\delta_r(t)] + f(T_r)[1-\exp(-a_r\delta_r(t))]\} \quad (2)$$

where $\delta_s(t)$ and $\delta_r(t)$ are the instantaneous thicknesses of the shocked and released layers during this time interval, respectively:

$$\delta_r(t) = \left(t-\frac{d}{U_s}\right)(U_r + u_{fs} - u_p)$$

$$\delta_s(t) = d\left(1-\frac{u_p}{U_s}\right) - \left(t-\frac{d}{U_s}\right)U_r \qquad \tau_{fs} < t < \tau_i$$

and τ_{fs} and τ_i are the time of arrival of the shock at the free

surface and time of arrival of the rarefaction at the driver-SiO_2 interface, respectively.

We can define time-dependent effective emissivities for each source:

$$\varepsilon_i(t) = r\varepsilon_i^0 \exp[-a_s\delta_s(t)] \exp[-a_u\delta_u(t)] \qquad 0 < t < \tau_{fs}$$

$$\varepsilon_i(t) = r'\varepsilon_i^0 \exp[-a_s\delta_s(t)] \exp[-a_r\delta_r(t)] \qquad \tau_{fs} < t < \tau_i$$

$$\varepsilon_s(t) = r\{1 - \exp[-a_s\delta_s(t)]\} \exp[-a_r\delta_r(t)] \qquad 0 < t < \tau_{fs}$$

$$\varepsilon_s(t) = r'\{1 - \exp[-a_s\delta_s(t)]\} \exp[-a_r\delta_r(t)] \qquad \tau_{fs} < t < \tau_i$$

$$\varepsilon_r(t) = 0 \qquad 0 < t < \tau_i$$

$$\varepsilon_r(t) = r'\{1 - \exp[-a_r\delta_r(t)]\} \qquad \tau_{fs} < t < \tau_i$$

where for times before shock arrival at the free surface the instantaneous thicknesses of shocked and unshocked layers are $\delta_s(t)$ and $\delta_u(t)$, respectively:

$$\delta_s(t) = t(U_s - u_p)$$
$$\delta_u(t) = d - tU_s \qquad 0 < t < \tau_{fs}$$

For the time interval of interest we can thus write (1) and (2) as

$$I(t) = \varepsilon_i(t)f[T_i(t)] + \varepsilon_s(t)f(T_s) + \varepsilon_r(t)f(T_r) \tag{3}$$

In order to determine T_s, *Lyzenga et al.* [1983] made the gray body assumption that $\varepsilon_s(\tau_{fs})$ is not a function of wavelength. They also made the tacit assumption that

$$\varepsilon_i(\tau_{fs})f[T_i(\tau_{fs})] \ll \varepsilon_s(\tau_{fs})f(T_s)$$

so that

$$I(\tau_{fs}) \simeq \varepsilon_s(\tau_{fs})f(T_s) \tag{4}$$

at each wavelength. By reading the experimental records at time τ_{fs}, experimental values were determined for the left-hand side of (4) for each of the six wavelengths, giving six equations and two unknowns, which were determined numerically.

We can approach the problem of solving for T_r similarly by making the gray body assumption for $\varepsilon_r(t_r)$ at some reading point $t_r > \tau_{fs}$ and by assuming that at this time, $I(t_r)$ is dominated by light from the released sample:

$$\varepsilon_i(t_r)f[T_i(t_r)] + \varepsilon_s(t_r)f(T_s) \ll \varepsilon_r(t_r)f(T_r)$$

so that

$$I(t_r) \simeq \varepsilon_r(t_r)f(T_r) \tag{5}$$

which can be solved just like (4).

The validity of the assumptions can be determined by fitting the observed time dependences to (1) and (2) and solving for a_s, a_r, ε_i^0, T_s, T_r, r, and r'. The functional form of $T_i(t)$ can be calculated as the solution of a one-dimensional heat conduction problem, as suggested by *Boslough* [1985]. All the other parameters are known or can be measured independently. *Svendson and Ahrens* [1987] outline a numerical method of solving a very similar problem for shocked MgO.

Lyzenga et al. [1983] observed that for SiO_2, $I(t)$ was approximately constant just before free surface arrival. One way of expressing this is

$$\frac{\tau_{fs}}{I(\tau_{fs})}\left(\frac{\partial I}{\partial t}\right)_{t=\tau_{fs}} \ll 1 \tag{6}$$

By differentiating (1) with respect to time and making the appropriate substitutions, one can show that in order for (6) to hold true the conditions,

$$a_s d \gg 0$$

and

$$a_u d \ll 1$$

are required. The second of these is independently known to be true for the starting material. The first condition implies that

$$\varepsilon_i(\tau_{fs}) \simeq 0 \qquad \varepsilon_s(\tau_{fs}) \simeq r$$

Similarly, one can show that if at some reading time $t_r > \tau_{fs}$, the intensity is approximately constant, then (if $T_r \neq T_s$) either

$$a_s\delta_s(t_r) \gg 0 \qquad a_r\delta_r(t_r) \ll 1$$

or

$$a_r\delta_r(t_r) \gg 0$$

The first set of conditions requires $I(t)$ to have a discontinuous change at $t = \tau_{fs}$, with the change in amplitude equal to r'/r, which would be expected to be only a few percent. Figure 1 shows that the change in $I(t)$ is much larger, so the second alternative is valid. This implies

$$\varepsilon_i(t_r) \simeq 0 \qquad \varepsilon_s(t_r) \simeq 0 \qquad \varepsilon_r(t_r) = r'$$

At the times of interest, (3) reduces to

$$I(\tau_{fs}) = rf(T_s) \tag{7}$$

$$I(t_r) = r'f(T_r) \tag{8}$$

One further assumption is required in order to estimate r and r': that the reflectivities of the shock front and the rarefaction wave are negligible. While we know of no direct measurement of shock reflectivities in SiO_2, estimates based on Gladstone-Dale type behavior and the known shock density limit reflectivities to less than 10%, assuming a perfect specular surface with zero tilt. By ignoring this reflectivity, our temperature calculations are slightly lower than the true temperatures. We can approximate r and r' by $1/R$, where R is the free surface reflectivity of unshocked SiO_2, a measured quantity almost independent of wavelength.

We can invert (7) and (8) and solve directly for the temperatures:

$$T_{s\lambda} = f^{-1}[RI_{\text{exp}}(\tau_{fs}, \lambda)]$$

$$T_{r\lambda} = f^{-1}[RI_{\text{exp}}(t_r, \lambda)]$$

where the wavelength dependence has been included explicitly and I_{exp} is the experimentally determined spectral radiance. T_s and T_r are taken to be the mean values of $T_{s\lambda}$ and $T_{r\lambda}$, and the standard deviation gives an estimate of measurement uncertainty.

Values of $I_{\text{exp}}(\tau_{fs}, \lambda)$ were taken directly from *Lyzenga* [1980], with a minor correction due to the fact that wavelength dependence of the turning mirror was previously neglected. These are the same corrections that were incorporated in the shock temperature calculations of *Ahrens et al.* [1982]. $I_{\text{exp}}(t_r, \lambda)$ was determined from the raw oscilloscope records of *Lyzenga* [1980], approximately 100 ns after τ_{fs}, when the intensity is nearly constant (cf. Figure 1). The temperatures determined in this way are tabulated in Table 1 and plotted in Figure 2. Postshock spectral radiances are given in Table 2

TABLE 1. Shock and Postshock Temperatures of SiO_2

P_H,* GPa	T_s, K	σ_{T_s}, K	T_r, K	σ_{T_r}, K	T_r, K
		α Quartz			
75.9	4440	40	...	...	...
85.9	4850	130	3660	40	4520
92.5	5430	120	3920	70	4870
99.3	5630	140	4000	80	4990
107.8	5900	200	...	...	...
109.7	6100	190	...	...	...
116.5	4910	110	3890	110	...
126.6	5320	90	4150	20	...
137.0	5760	90	...	...	...
		Fused SiO_2			
58.9	4960	90	3740	50	4450
68.5	5110	70	...	...	...
73.3	4620	80	3910	50	...
81.2	5080	70	...	...	...
93.2	5770	120	...	...	...
104.2	6530	170	...	...	...
109.9	7080	220	...	...	...

*Shock pressure [*Lyzenga et al.*, 1983].

and plotted in Figure 3 along with the best fitting Planck distribution functions.

The absorption coefficient a_r can be estimated for one experiment from the data in Figure 1 using (5) for a reading time of $t_r = \tau_{fs} + \Delta t$. Figure 1 depicts the spectral radiance history for 650-nm light radiated from fused silica shocked to 73.3 GPa [*Lyzenga et al.*, 1983]. According to Figure 1, for $\Delta t > 30$ ns, $I(t)$ is approximately constant. Assuming a release wave speed of about 10 km/s provides the constraint $a_r(\lambda = 650) \gg 300\ \text{mm}^{-1}$, which implies that the released silica becomes opaque on the time scale of the experiments.

There are a number of criticisms which could be made of the above model, and those should be addressed. Some of the problems are discussed by *Zel'dovich and Raizer* [1967] in the context of phenomena associated with the emergence of a shock wave at the free surface of a solid. First is the tacit implication that the material remains intact, homogeneous, uniform, and under uniaxial strain as it releases to zero pressure. One would expect some sort of disruption (i.e., spall, fragmentation, or "fluff") to occur at the free surface. However, even if the distribution of mass and velocity of the released material is nonuniform, the temperature of the individual fragments should be the same since they are all at or near the same pressure. The effect of fragmentation would be the introduction of numerous surfaces and interfaces which would act as scattering centers. This would have an effect on the value of the absorption coefficient a_r in (2) and subsequent equations, but the model is still valid for a reasonable size range of fragments. If the fragments are too small ($\lesssim 0.1$ μm), Rayleigh scattering will occur, and a_r will exhibit wavelength dependence. The spectral radiances at the various wavelengths would then have different time dependences and would approach their asymptotic values at different rates. If they are all measured after they reach their final values, the temperature determinations are still valid. If the fragments are too large (a significant fraction of the photodetector image size; in this case, about 1 mm) the differential motions and rotations of the fragments would generate fluctuations in scattered light intensity. No such fluctuations were observed in the spectral radiances examined in this study.

Another possible problem is the treatment of the rarefaction wave as a discontinuity. A more general model would have to consider the fact that there is a temperature gradient and, in general, a gradient in the material absorption coefficient along the rarefaction front. If the released layer becomes optically thick, the gradient no longer matters, as light from the rarefaction zone is not detected. However, if released material is transparent, a much more complicated radiative transport model is required. In this case, a continuum model replaces the three-layer model presented here. In such a model a continuum of temperatures radiates light, and there is a time- and temperature-dependent effective emissivity. Because a range of temperatures is observed simultaneously, the spectral radiance as a function of wavelength would not be expected to approximate a single-temperature Planck function as is observed in the present data. This more general model is beyond the scope of this paper and will not be developed here. However, some attention should be given to a special case that provides an alternative explanation for the postshock spectral radiance data under consideration.

According to the release data of *Chhabildas and Miller* [1985] there is a sharp bend in the release path which implies a sudden conversion from high-density to low-density silica. It is conceivable that this conversion is accompanied by a discontinuity in the absorption coefficient; in particular, the high-density silica is opaque and the low-density (released) silica is transparent. In this case the observed light would be radiated from an interface between the two states, and the associated temperature would correspond to the partial release state. While there is no information in the present data to preclude this alternative, it is based on more specific assumptions than the former explanation. The following discussion is based on the measured postshock temperatures corresponding to the final release state, though the possibility that they could be partial release states should be kept in mind.

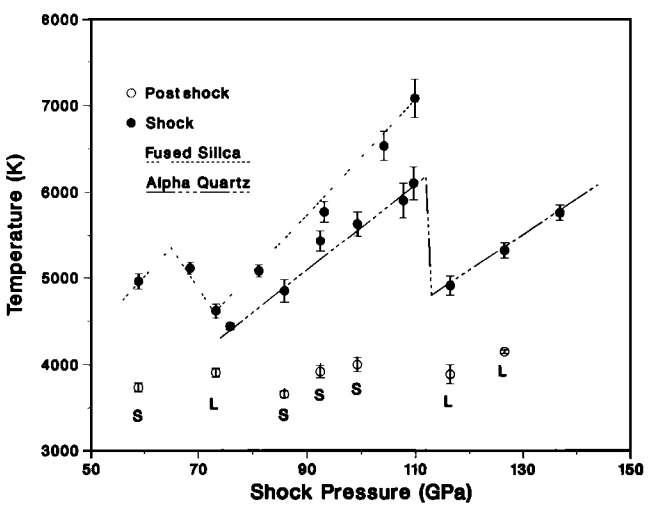

Fig. 2 Measured shock and postshock temperatures for silica. Solid symbols are shock temperatures, and open symbols are corresponding postshock temperatures; both sets are plotted as a function of shock pressure. Error bars indicate standard deviation in brightness temperature determined at each of six wavelengths. They do not carry information about experimental error. "S" and "L" label states inferred to have released from solid stishovite and liquid silica shock states, respectively.

TABLE 2. Postshock Spectral Radiance Data

Wavelength, nm	Spectral Radiance, 10^{12} W/m^2 sr						
	Fused Silica		α Quartz				
	P=58.9	P=73.3	P=85.9	P=92.5	P=99.3	P=116.5	P=126.6
450.2	1.38	1.75	1.10	2.37	2.79	1.92	2.95
507.9	2.09	2.52	1.66	2.67	3.15	2.68	3.73
545.1	2.17	2.62	1.69	2.84	3.28	2.84	4.36
598.0	2.35	3.14	1.96	3.12	3.58	2.23	4.61
650.0	2.71	3.86	2.54	3.54	3.64	3.86	5.18
792.0	2.72	4.04	2.76	3.43	3.88	3.66	4.83

P is shock pressure in gigapascals.

DISCUSSION

As seen in Figure 2, the temperature-pressure Hugoniots of both fused silica and α quartz consist of two segments of increasing temperature, separated by a marked drop in temperature over a short pressure range. The interpretation of *Lyzenga et al.* [1983] is that these temperature drops represent the shock-induced melting of stishovite. They point out that because the two segments of negative slope do not connect to make a continuous curve, they do not delineate an equilibrium coexistence curve between the two phases. They propose that instead, the phase transformation is "overdriven" by the shock, and metastable stishovite exists on both Hugoniots in the liquid silica phase region. At a sufficiently high pressure on the Hugoniot the shock is strong enough to melt the silica. This appears on the PT Hugoniot as a sharp drop in temperature because the melting is an endothermic transformation. Thus at shock pressures just below the temperature drop the state consists of metastable stishovite; at pressures above the drop the state is liquid silica in phase equilibrium. This view is supported by the α quartz data of *Chhabildas and Miller* [1985], who found a decrease in sound speed between 71 and 108 GPa. The higher pressure is close to that over which the shock temperature decreases in α quartz (Figure 2).

For the liquid silica Hugoniot states above the temperature drop the release paths would not be expected to cross any phase boundaries, and in the absence of dissociation or vaporization the final release state (at zero pressure) should also be liquid silica. Three postshock temperatures corresponding to release from these states have been determined, and all are at temperatures near 4000 K, which is well above the zero-pressure melting point of quartz. It is also above the quartz boiling temperature, so at some point on the release path the liquid should begin to boil if thermodynamic equilibrium were maintained. However, according to *Zel'dovich and Raizer* [1967 p. 764] the formation of nuclei of the new phase (vapor bubbles) ". . . requires a rather large activation energy to destroy the continuity of the material and to form the bubble surfaces." At temperatures of up to thousands of degrees, the rate of this process ". . . is so negligibly small that actually the solid continues to expand and cool down to zero pressure

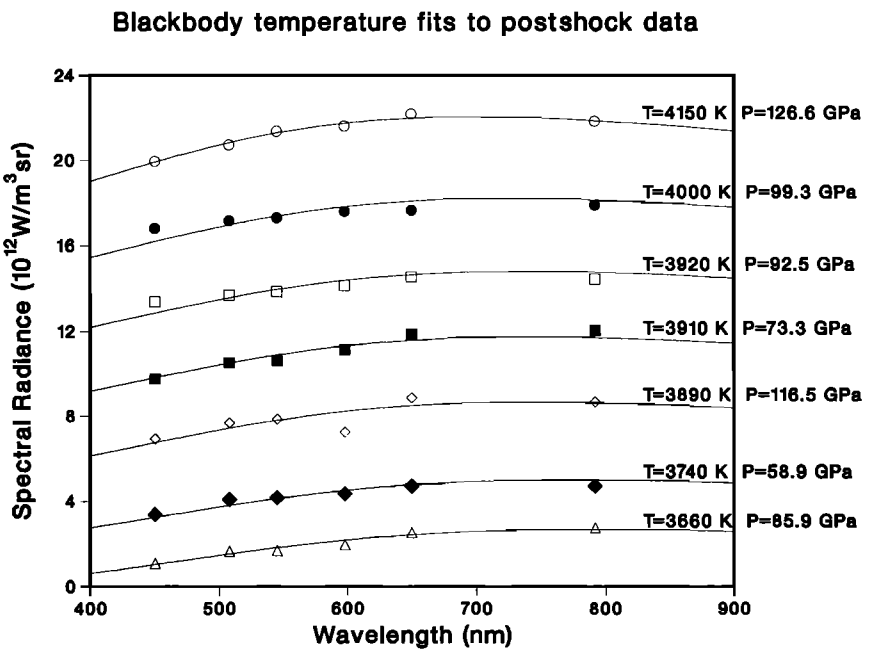

Fig. 3. Spectral radiance data used to determine post-shock temperatures, plotted with the best fitting blackbody curves. Each set of data is vertically offset by 2 × 10^{12} W/m^2 sr more than the data set immediately beneath it for plotting purposes. The lowest data set is not offset.

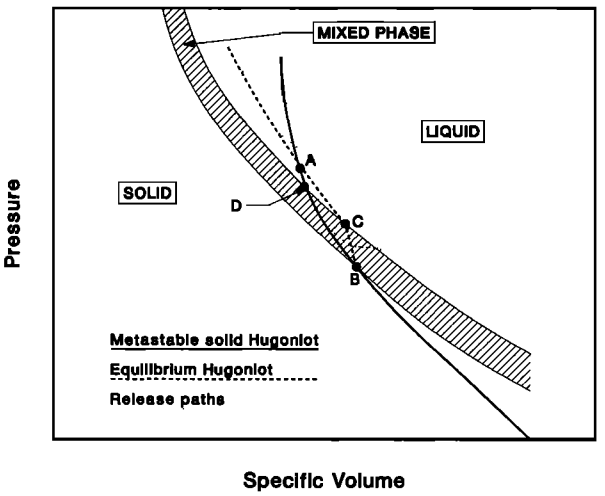

Fig. 4. Schematic diagram of high-pressure silica phase diagram, showing hypothetical Hugoniots and release paths. The solid curve corresponds to the Hugoniot in which the shock state is stishovite, metastable above point B. The dashed curve is the Hugoniot in which shock states are in-phase equilibrium. Dotted curves are release paths. The shaded area is the mixed phase region where stishovite and liquid coexist in equilibrium.

along the 'superheated liquid' isentrope . . ." If we make the assumption that the release is entirely isentropic, then the postshock temperature of the superheated liquid phase is given by

$$T_R = T_H \exp\left(\int_{V_R}^{V_H} [\gamma(V)/V]\, dV\right) \tag{9}$$

where $\gamma(V)$ is the thermodynamic Grüneisen parameter. The unknowns in (9) are V_R and the function $\gamma(V)$. T_H and T_R are measured temperatures, and V_H can be determined from the known shock and particle velocities [see *Lyzenga et al.*, 1983, Table 3] using the Rankine-Hugoniot equations. We can invoke the frequently made assumption that $\gamma(V)/V$ is constant to reduce (9) to a linear equation in two unknowns:

$$V_H = V_R - \frac{V}{\gamma(V)} \ln\left[\frac{T_H}{T_R}\right]$$

which can be solved as a linear regression problem for V_R and $\gamma(V)/V$ using the three pairs of shock/postshock temperature data points corresponding to release within the silica liquid region of stability. The result of this fit gives the specific volume on release of $V_R = 0.266 \pm 0.003 \text{m}^3/\text{Mg}$ ($\rho_R = 3.76 \pm 0.05$ Mg/m^3). This density is significantly less than the "zero-pressure density" of 4.15 Mg/m^3 used by *Lyzenga et al.* [1983] but would correspond to a thermal expansion of about 11% over nearly 4000 K, which is not unreasonable. The Grüneisen parameter given by the present fit is $\gamma(V)/V = 3.5 \pm 0.7$ Mg/m^3, which is significantly less than the value used by *Lyzenga et al.* [1983]. However, those workers determined $\gamma(V)$ from consideration of fused silica and α quartz Hugoniot data in the liquid regime, and they point out that the γ parameters that they use are only loosely constrained by the data. To check the present Grüneisen parameter for consistency, it would be useful to have more release path data centered in the high-pressure liquid regime to compare to the one path of *Chhabildas and Miller* [1985].

The relationship between the other four shock/postshock temperature pairs (labeled "S" in Figure 2) presented here is much more complicated and cannot be expressed by a single equation such as (9). In order to describe how such a calculation could be done, it is necessary to go into a detailed account of how the shocked material releases to zero pressure. The present interpretation of the data is very similar to that of *Lyzenga et al.* [1983] but differs somewhat in detail. These details are illustrated in Figure 4, which is a plot of the α quartz Hugoniot in the region where it crosses the inferred stishovite/liquid mixed phase regime in the P-V plane. Actually, two Hugoniots are plotted: the dashed curve corresponds to shock states that are in phase equilibrium, and the solid curve is the extension of the Hugoniot that corresponds to metastable stishovite in the shocked state.

The data are consistent with a true Hugoniot that follows the stishovite curve through the mixed phase regime and at point A, where the curves cross, converts to the stable liquid Hugoniot. The pressure at point A is that at which the drop in shock temperature is observed in the PT plane (Figure 2). *Lyzenga et al.* [1983] apparently suggest that this point defines the upper boundary of the mixed phase region, but a geometric argument based on Figure 4 shows that it must actually lie above. Where the two curves diverge at point B, the stable curve must have a steeper slope than the stishovite curve, since there is a positive volume change on melting. At point C the stable curve exits the mixed phase region and must change slope. The slope must be shallower than the stishovite curve, since the liquid is more compressible, but it must be steeper than the phase boundary, or it would cross back into the mixed phase regime. Therefore the curves must intersect, and the point of intersection must lie above the phase boundary. The resultant cusp in the true Hugoniot is still consistent with the transition region in the shock velocity-particle velocity data, as pointed out by *Lyzenga et al.* [1983]. There is no a priori reason why the transformation would be expected to occur at point A, except that at any other point the true Hugoniot would have a discontinuity in density and at point A the Hugoniot is continuous but its slope is discontinuous.

In order to do a rigorous calculation of the postshock temperature one must consider all the possible paths by which the material could release through the mixed phase region. Since the various paths are not well constrained and the appropriate thermodynamic constants for each phase are not well known, such a calculation is too complicated to give useful answers without making gross simplifications. In the following discussion the possible true unloading paths are qualitatively described, but no attempt is made to use them to relate shock and postshock temperatures.

There are three possible paths by which the material can release from a stishovite shock state to a liquid release state. The first is from pressures below the cusp (A) but above some point D on the metatable stishovite Hugoniot. According to *Duvall and Graham* [1977], if the pressure is sustained until phase equilibrium is achieved, the first segment of release will be along some path to the equilibrium Hugoniot. They suggest this nonequilibrium melting will occur along the Rayleigh line, basing this supposition on the assumption of a steady decay in the shock profile, which has not been observed in silica. It seems reasonable that the nonequilibrium melting would occur isochorically due to inertial constraint. At pressures above some point D there is a sufficient amount of energy in the metastable stishovite to cause total melting, so this first releases to a point within the liquid region of stabili-

ty. The second step releases from this point to the final state through a single equilibrium phase and can be described by (9) (where V_H and T_H are now taken to be the values at this intermediate state).

The second possible release path is centered on stishovite states between points B and D. For this region there is insufficient shock energy to completely melt the stishovite, but partial melting can occur. If we again assume that this metastable melting occurs along an isochore, the first step takes the material to a state within the mixed phase region. Once equilibrium is achieved, the material can release through the mixed phase region, continuing to melt in equilibrium until the upper phase boundary is reached, whereupon its final release step is again described by (9).

The third release path also follows three steps. For stishovite at shock states below point B the entire release occurs in equilibrium. The first step releases through solid stishovite (possibly crossing a solid-solid phase boundary into the field of one of the low-pressure polymorphs) until the lower solid-liquid phase boundary is reached. The second step is equilibrium melting, and the final step releases through the liquid phase region as before.

Clearly, with so many possible types of release paths from the stishovite phase, the calculation of postshock temperature is much more complicated. One can immediately see that the differences between shock and postshock temperature is greater for release inferred from stishovite (marked by "S" in Figure 2) than for release from liquid (marked by "L" in Figure 2). The excess temperature of the superheated stishovite decreases as the thermal energy goes to the latent heat of melting, which is an endothermic transformation.

Rather than attempting to calculate postshock temperatures by such complicated means, it is informative to use measured postshock temperatures to constrain independently the high-pressure melting temperature. The final step in all three types of release paths is the same: isentropic decompression from some point on the liquid side of the melting curve, through the liquid phase to the final release state. The postshock temperature depends on the intermediate temperature T_i and specific volume V_i through (9), where the Hugoniot variables are replaced by these intermediate values. Because this release step takes place entirely through the liquid phase, we can use the $\gamma(V)/V$ determined above. Because the measured postshock temperatures are all within a few hundred degrees of one another, we can also use the previously determined value for V_R. We can put a lower bound on V_i; its minimum value of V_H corresponds to complete nonequilibrium melting along an isochore. Since T_i is greater than or equal to the melting temperature at the pressure of the intermediate state, we can write

$$T_m(P_i) \leq T_R \exp\,[3.46(0.266 - V_H)]$$

These upper bounds to the melting temperature range from about 4500 to 5000 K and monotonically increase with pressure (Table 1), in agreement with the interpretation of *Lyzenga et al.* [1983]. The volume V_i may be greater than V_H by an amount comparable to the volume change on melting (ΔV_m) for complete equilibrium melting due to partial release along the melting curve. If the *Lyzenga et al.* [1983] value $\Delta V_m/V = 0.027$ is added, the melting temperature estimates decrease by about 100 K. In any case, the measured postshock temperatures are not inconsistent with the model that was described by *Lyzenga et al.* [1983]: that the melting curve has a positive slope and lies in the high 4000 K temperature range for pressures between 60 and 100 GPa.

Since there is evidence from the data of *Chhabildas and Miller* [1985] that there is a sharp band in the release path (implying a conversion from high- to low-density liquid silica), the simplification used in the radiation transport model treating the rarefaction wave as a discontinuity may be invalid, as previously mentioned. If opaque material suddenly becomes transparent when the high- to low-density conversion takes place, then these "postshock" temperatures correspond to a partial release state and not a final (ambient pressure) state. If this is indeed the case, T_R and V_R in (9) and subsequent equations correspond to this partial release state. The calculations making use of these equations are still valid.

CONCLUSIONS

By considering measured spectral radiance of light radiated from samples which have been shocked and allowed to release to zero pressure, residual (postshock) temperatures have been determined, although there is some ambiguity as to whether the temperature corresponds to a partial or final release state. The same type of radiative energy transport models that describe the time dependence of shock-induced radiation of light can be extended to apply to the postshock regime. The measured postshock temperatures, when combined with measured shock temperatures, have been used to determine Grüneisen parameter and postshock specific volume. In principle, they can also be used to detect or confirm the existence of phase transformations and determine the temperatures along the coexistence curve.

In the case of SiO_2, postshock temperatures are consistent with the interpretation based on shock temperatures alone: that stishovite melts at about 4500 K at 70 GPa and the melting curve has a shallow, positive slope. Calculations based on the measured shock and postshock temperatures give a Grüneisen parameter of high-pressure, liquid silica of $\gamma(V) = 3.5V$, and a postshock specific volume of $V_r = 0.266$ cm^3/g at a temperature of about 4000 K, although there is still uncertainty as to whether this corresponds to a partial or final release state. All these values except the Grüneisen parameter are consistent with those of *Lyzenga et al.* [1983]; however, $\gamma(V)$ does not have a major influence on the interpretations.

Acknowledgments. I would like to thank T. J. Ahrens, G. A. Lyzenga, A. C. Mitchell, and W. J. Nellis for allowing me to use their unpublished spectral radiance data. L. C. Chhabildas provided helpful comments during the writing of the manuscript. This work was performed at Sandia National Laboratories supported by the U.S. Department of Energy under contract DE-AC04-76DP00789.

REFERENCES

Ahrens, T. J., G. A. Lyzenga, and A. C. Mitchell, Temperatures induced by shock waves in minerals: Applications to geophysics, in *High-Pressure Research in Geophysics*, edited by S. Akimoto and M. H. Manghnani, pp. 579–594, Center for Academic Publications Japan, Tokyo, 1982.

Boslough, M. B., A model for time dependence in shock-induced thermal radiation of light, *J. Appl. Phys.*, *58*, 3394–3399, 1985.

Chhabildas, L. C., and J. M. Miller, Release-adiabat measurements in crystalline quartz, Sandia *Rep. SAND85-1092*, Sandia Natl. Lab., Albuquerque, N. M., 1985.

Duvall, G. E., and R. A. Graham, Phase transitions under shock-wave loading, *Rev. Mod. Phys.*, *49*, 523–579, 1977.

Lyzenga, G. A., Shock temperatures of materials: Experiments and applications to the high pressure equation of state, Ph.D. thesis, Calif. Inst. of Technol., Pasadena, 1980.

Lyzenga, G. A., and T. J. Ahrens, Multiwavelength optical pyrometer for shock compression experiments, *Rev. Sci. Instrum.*, *50*, 1421–1424, 1979.

Lyzenga, G. A., T. J. Ahrens, and A. C. Mitchell, Shock temperatures

of SiO_2 and their geophysical implications, *J. Geophys. Res.*, *88*, 2431–2444, 1983.

McQueen, R. G., J. N. Fritz, and S. P. Marsh, On the equation of state of stishovite, *J. Geophys. Res.*, *68*, 2319–2322, 1963.

Nicol, M., S. W. Johnson, and N. C. Holmes, Shock-chemistry of benzene studied by spectra from and behind the shock front, in *Shock Waves in Condensed Matter—1987*, edited S. C. Schmidt and N. C. Holmes, pp. 471–476, North-Holland, New York, 1988.

Raikes, S. A., and T. J. Ahrens, Post-shock temperatures in minerals, *Geophys. J. R. Astron. Soc.*, *58*, 717–747, 1979.

Rice, M. H., R. G. McQueen, and J. M. Walsh, Compressibility of solids by strong shock waves, *Solid State Phys.*, *6*, 1–63, 1958.

Stevens, A. L., and O. E. Jones, Radial stress release phenomena in plate impact experiments: Compression-release, *J. Appl. Mech.*, *39*, 359–366, 1972.

Svendson, B., and T. J. Ahrens, Shock-induced temperatures of MgO, *Geophys. J. R. Astron. Soc.*, *91*, 667–691, 1987.

Wackerle, J., Shock-wave compression of quartz, *J. Appl. Phys.*, *33*, 922–937, 1962.

Zel'dovich, Ya. B., and Yu. P. Raizer, *Physics of Shock Waves and High-Temperature Hydrodynamic Phenonema*, pp. 762–778, Academic, Orlando, Fla., 1967.

M. B. Boslough, Division 1131, Sandia National Laboratories, Albuquerque, NM 87185.

(Received June 15, 1987;
revised November 20, 1987;
accepted February 10, 1988.)